Hydrothermal Synthesis and Characterization of Sodium Manganese Oxo-Phosphate $Na_2Mn_2O(PO_4)_2 \cdot H_2O$

Wei Tong,[†] Guan-Guang Xia,[‡] Zheng-Rong Tian,[†,⊥] Jia Liu,[‡] Jun Cai,[†] Steven L. Suib,*[,†,‡,§] and Jonathan C. Hanson[||]

Department of Chemistry, U-3060, Institute of Materials Science, and Department of Chemical Engineering, University of Connecticut, Storrs, Connecticut 06269, and Chemistry Department, Brookhaven National Laboratory, Upton, New York 11973

Received June 4, 2001. Revised Manuscript Received November 2, 2001

Sodium manganese oxo-phosphate $Na_2Mn_2O(PO_4)_2 \cdot H_2O$ (MPOS-3) has been prepared in single-crystal and polycrystalline forms by hydrothermal methods. The crystal structure was determined from a $15 \times 15 \times 80$ μm crystal with synchrotron radiation. In the structure, zigzag edge-sharing MnO_6 octahedral chains are connected by PO_4 tetrahedra to form two-dimensional planes. A second PO_4^{3-} group sticks out of the planes by sharing three apexes with three MnO_6 octahedra of a zigzag chain. The fourth apex of this PO_4^{3-} groups interacts strongly with sodium ions that are located between the two-dimensional planes. The sodium ions are exchangeable. Ion exchanging half of the Na^+ with Ca^{2+} expands the surface area from 17 to 45 m^2/g. MPOS-3 loses water at about 220 °C. The dehydrated form is stable up to 550 °C, above which O_2 is liberated. The FTIR spectrum shows two distinct −OH stretching vibration bands, one at 3627 cm^{-1} and another at 3437 cm^{-1}. MPOS-3 also demonstrates catalytic activity in oxidation of 2-propanol by air to produce acetone. Carbon dioxide is the only byproduct. Preliminary results show 27% conversion of 2-propanol at 450 °C with 65% selectivity toward acetone.

I. Introduction

Transition-metal-containing zeolite-like materials are of both academic and practical interest since the combination of the open-structure characteristics of zeolites and transition-metal chemistry will give rise to unique functionalities, which can be utilized in catalytic, separation, electronic, and magnetic applications. Many open-structural transition-metal phosphates such as cobalt,[1,2] vanadium,[3−5] molybdenum,[6] and iron[7] phosphates have been reported.

Manganese has the most varied oxidation states of all the elements. Materials of Mn^{3+} or Mn^{4+} or both are widely used in batteries[8] and catalytic processes.[9−12] However, reported manganese phosphates with open structures often contain only Mn^{2+}.[13,14] One reason is the easy reduction of Mn^{3+} and/or Mn^{4+} materials to Mn^{2+} materials at high temperature. The other reason is the very low solubility of Mn^{3+} and Mn^{4+} in solution, which causes difficulties in the hydrothermal synthesis of open-structural materials with high crystallinity.

To alleviate this problem, phosphate groups can be introduced via hydrothermal syntheses of manganese materials. Phosphate groups coordinate to Mn^{3+} at a pH ∼ 6−7, which may slow nucleation processes and therefore may allow more controllability of hydrothermal syntheses. A family of new manganese (oxo- and/or hydroxo-) phosphates has been prepared with this approach. MPOS-3 is one of these materials. The structure of MPOS-3 is layered with Na^+ residing between the octahedral−tetrahedral layer of MnO_6 and PO_4. Ion exchanging half of the Na^+ with Ca^{2+} expands the surface area from 17 to 45 m^2/g. Dehydrated MPOS-3 is stable up to 550 °C. MPOS-3 also shows activity in the catalytic reaction of 2-propanol and oxygen.

* To whom correspondence should be addressed.
[†] Department of Chemistry, University of Connecticut.
[‡] Institute of Materials Science, University of Connecticut.
[§] Department of Chemical Engineering, University of Connecticut.
[||] Brookhaven National Laboratory.
[⊥] Current address: Institute of Materials Science, University of California at Davis.

(1) Chen, J.-S.; Jones, R. H.; Natarajan, S.; Hursthouse, M. B.; Thomas, J. M. *Angew. Chem., Int. Ed. Engl.* **1994**, *33*, 639−640.
(2) Feng, P.; Bu, X.; Stucky, G. D. *Nature* **1997**, *388*, 735−741.
(3) Zhang, Y.; Warren, C. J.; Clearfield, A.; Haushalter, R. C. *Polyhedron* **1998**, *17*, 2575−2580.
(4) Lu, Y.; Haushalter, R. C.; Zubieta, J. *Inorg. Chim. Acta* **1998**, *268*, 257−261.
(5) Haushalter, R. C.; Chen, Q.; Soghomonian, V.; Zubieta, J.; O'Connor, C. J. *J. Solid State Chem.* **1994**, *108*, 128−133.
(6) Soghomonian, V.; Meyer, L. A.; Haushalter, R. C.; Zubieta, J. *Inorg. Chim. Acta* **1998**, *275−276*, 122−129.
(7) DeBard, J. R. D.; Reiff, W. M.; Warren, C. J.; Haushalter, R. C.; Zubieta, J. *Chem. Mater.* **1997**, *9*, 1994−1998.
(8) Chabre, Y.; Pannetier, J. *Prog. Solid State Chem.* **1995**, *23*, 1−130.
(9) Krishnan, V. V.; Suib, S. L. *J. Catal.* **1999**, *184*, 305−315.
(10) Wang, J.-Y.; Xia, G.; Yin, Y.-G.; Suib, S. L.; O'Young, C. L. O. *J. Catal.* **1998**, *176*, 321−328.
(11) Xia, G. G.; Yin, Y. G.; Willis, W. S.; Wang, J. Y.; Suib, S. L. *J. Catal.* **1999**, *185*, 91−105.
(12) Luo, J.; Zhang, Q.; Huang, A.; Suib, S. L. *Microporous Mesoporous Mater.* **2000**, *35−36*, 209−217.
(13) Daidouh, A.; Martinez, J. L.; Pico, C.; Veiga, M. L. *J. Solid State Chem.* **1999**, *144*, 169−174.
(14) Escobal, J.; Mesa, J. L.; Pizarro, J. L.; Lezama, L.; Olazcuaga, R.; Rojo, T. *J. Mater. Chem.* **1999**, *9*, 2691−2695.

10.1021/cm010540a CCC: $22.00
Published on Web 01/18/2002

Table 1. Summary of Crystallographic and Refinement Data for MPOS-3

compound	$Na_2Mn_2O(PO_4)_2 \cdot H_2O$
crystal system	monoclinic
space group	$P2(1)/m$
a	7.793(2) Å
b	6.889(1) Å
c	8.526(2) Å
β	109.15(3)°
Z	2
V	451.9 Å^3
T	298 K
D_c	2.79 cm^3/g
λ	0.93760 Å
no. of reflections	592
no. of parameters	89
$R(f) = \sum\|F_{obs} - F_{calc}\|/\sum F_{obs}$	0.0267
GOF	0.955

II. Experimental Section

Materials. All chemicals were used as received with no further purification. Manganese sulfate monohydrate was bought from Fisher. Sodium hexametaphosphate and phosphorus acid (86.8%) were purchased from Baker. Sodium permanganate monohydrate (97%) and 2-butanol (99.5%) were obtained from Fluka. Tetraethylammonium bromide (98%) was purchased from Alfa.

Synthesis. Solution A was made by dissolving 0.14 mol of $MnSO_4 \cdot H_2O$, 0.45 mol of $(NaPO_3)_6$, and 0.023 mol of H_3PO_4 in 31.3 mL of deionized water. Solution B was made by dissolving 0.35 mol of $NaMnO_4 \cdot H2O$ in 14.8 mL of deionized water. After mixing solutions A and B, 0.40 mol of $(C_2H_5)_4NBr$ was added to the mixture. Then 90.0 mL of 2-butanol was added. The whole mixture was aged at room temperature for 3 weeks. The gel was separated for autoclaving in a tetrafluoroethylene-lined vessel at 150 °C for 7 days. The fine powder obtained was washed a few times with deionized water. This fine powder is the polycrystalline form of MPOS-3.

Ion Exchange. MPOS-3 is refluxed with 2 M $CaCl_2$ aqueous solution (v/w = 20) at 90 °C for 3−4 h. After the solution is washed and filtrated with deionized water, the same reflux procedure is repeated one more time. Half of the Na^+ is exchanged with Ca^{2+} by this procedure, as determined by ICP-AES.

Single-Crystal Crystallography. Diffraction data were collected at synchrotron beamline X7B of NSLS at Brookhaven National Laboratory from an 80 × 15 × 15 μm crystal. Rotation methods were used. The data were recorded on a MAR345 image plate (150-μm pixels). The wavelength and detector distance were calibrated from a LaB_6 powder pattern using the FIT2D program.

Two full hemispheres of data were collected. The first has a longer exposure time to obtain the weak diffraction and consequently some of the diffraction data were saturated. Therefore, a second data set was collected with a much shorter exposure time. The intensity of diffraction was extracted and scaled with the DENZO program.[15] There were 7255 data points collected that merged to 592 diffraction with R_{merge} = 0.057. The orientation matrix and unit cell parameters were also determined with the DENZO program. The unit cell was determined separately for each recorded image. The unit cell parameters given in Table 1 are the mean values, and the estimated standard deviations came from an analysis of the repeatability. The structure solution[16] and refinement[17] were performed with Brucker SHELXTL. All estimated standard deviation in bond lengths, bond angles, and torsion angles are calculated from the full co-variance matrix.

Elemental Analysis. A Perkin-Elmer model 140 atomic emission spectrometer with inductively coupled plasma (ICP-AES) was used to determine the total manganese, sodium, and phosphorus concentration. The solid sample was dissolved in concentrated hydrochloric acid, which was then diluted with deionized water for the analysis.

Powder X-ray Diffraction (XRD). A Scintag XDS-2000 diffractometer with Cu Kα radiation was used to collect diffraction patterns. About 0.3 g of MPOS-3 powder was side-packed into an aluminum sample holder for data collection.

Fourier Transform Infrared Spectrum (FTIR). Transmittance FTIR spectra were collected with a Nicolet Magna-IR model 750. A mercury−cadmium−telluride (MCT-B) detector and a KBr beam splitter were used. The solid sample was mixed with KBr (∼1 wt %) and pressed into a pellet for data collection.

Thermogravimeteric Analysis (TGA). A TA Instrument Model 2950 was used for thermal stability analysis. The TGA experiment was conducted under a N_2 atmosphere (10 mL/min) with a temperature ramping rate of 10 °C/min.

Temperature-Programmed Desorption (TPD). TPD analysis was employed to detect the decomposition species of the sample upon heating. The experiment was performed on a lab-designed setup with an Omega CN 2042 temperature-programmed controller. About 20 mg of sample was purged and then heated in flowing He to 700 °C with a ramping rate of 10 °C/min. The decomposition species were analyzed with a MKS-UTI PPT quadrupole mass spectrometer.

Specific Surface Area and Pore Size Distribution. A Micromeritics ASAP 2010 was used to perform adsorption/desorption experiments with nitrogen as the adsorbate at liquid N_2 temperature. Specific surface areas were calculated by the BET method. A two-step method is adapted for adsorption measurements to avoid helium trapping, so that calculations of micropore size distribution would not be affected.

Catalytic Activity Test. The catalytic reactions were performed in a fixed bed reactor at 450 °C and 1 atm pressure. The GHSV is 1.44×10^4, which is composed of 1 part of air and 5 parts of helium. The 2-propanol concentration was 7670 ppm and 50 mg of MPOS-3 was used. The products were quantified with a Hewlett-Packard Model 5890II GC with a carboxen 1006 plot column and a TCD detector for carbon dioxide analysis and a DB-1 column and a FID detector for organic component analysis.

III. Results

A. Synthesis. The initial pH of the precursor mixture is adjusted to be between 3 and 4. Adding 2-butanol facilitates the formation of the product. Tetraethylammonium cations (TEA^+) are not included in the final structure of MPOS-3. Enough aging time is allowed to obtain a gel with the desired composition. However, MPOS-3 single crystals were obtained as impurities of a poorly crystalline manganese oxide phase if no TEABr and 2-butanol were added. These single crystals were used for atomic structure determination by single-crystal crystallography. Polycrystalline MPOS-3 was used for all other characterizations.

B. Crystalline Structure Analysis. The MPOS-3 space group was determined to be $P2_1/m$. There are two kinds of crystallographic positions for manganese and phosphorus. According to the bond length and bond angle data in Table 2, all manganese ions have an elongated octahedral environment due to Jahn−Teller effects, whereas the $Mn(1)O_6$ octahedra are more distorted in terms of bond angles.

As shown in Figure 1, each MnO_6 octahedron shares two edges with two other MnO_6 octahedra to form a zigzag chain. The two edges provided by $Mn(1)O_6$ have a common oxygen ion, which can be considered to be a reason for the distortion of $Mn(1)O_6$ octahedra. The

(15) Otwinowski, Z.; Minor, W. *Methods Enzymol.* **1997**, *276*, 307−326.
(16) Sheldrick, G. M. *Acta Crystallogr.* **1990**, *A46*, 467−473.
(17) Sheldrick, G. M. FIT2D Program. ESRF Internal Report, 1993.

Table 2. Selected Bond Lengths (Å) and Bond Angles (deg) for MPOS-3

$Mn(1)O_6$ octahedron		$Mn(2)O_6$ octahedron	
Mn(1)−O(9)	1.885(4)	Mn(2)−O(6)/O(6^{ii})	1.929(3) ×2
Mn(1)−O(5)	1.904(4)	Mn(2)−O(9)/O(9^{ii})	1.909(2) ×2
Mn(1)−O(3)	1.953(4)	Mn(2)−O(8)/O(8^{ii})	2.251(3) ×2
Mn(1)−O(2)	1.991(4)	O(6)−Mn(2)−O(8)	90.29(12)
Mn(1)−O(8^{i})/O(8)	2.223(3) ×2	O(8^{ii})−Mn(2)−O(9)	99.31(12)
O(8^{i})−Mn(1)−O(3)	98.54(7)	O(8^{ii})−Mn(2)−O(9^{ii})	80.69(12)
O(9)−Mn(1)−O(8^{i})	81.96(7)		
O(2)−Mn(1)−O(3)	74.28(17)		
O(8)−Mn(1)−O(2)	93.80(8)		

Na^+ to oxygen distances	
Na−O(4)	2.258(3)
Na−O(3^{v})	2.409(3)
Na−O(2^{vi})	2.465(3)
Na−O(6^{vii})	2.387(3)

symmetry codes:
i = $x, -y + 1/2, z$
ii = $-x + 1, y, z + 1$
iii = $-x + 2, y + 1/2, -z + 1$
iv = $-x + 2, -y, -z + 1$
v = $-x + 2, -y, -z + 2$
vi = $x, y, z + 1$
vii = $-x + 1, -y, -z + 2$

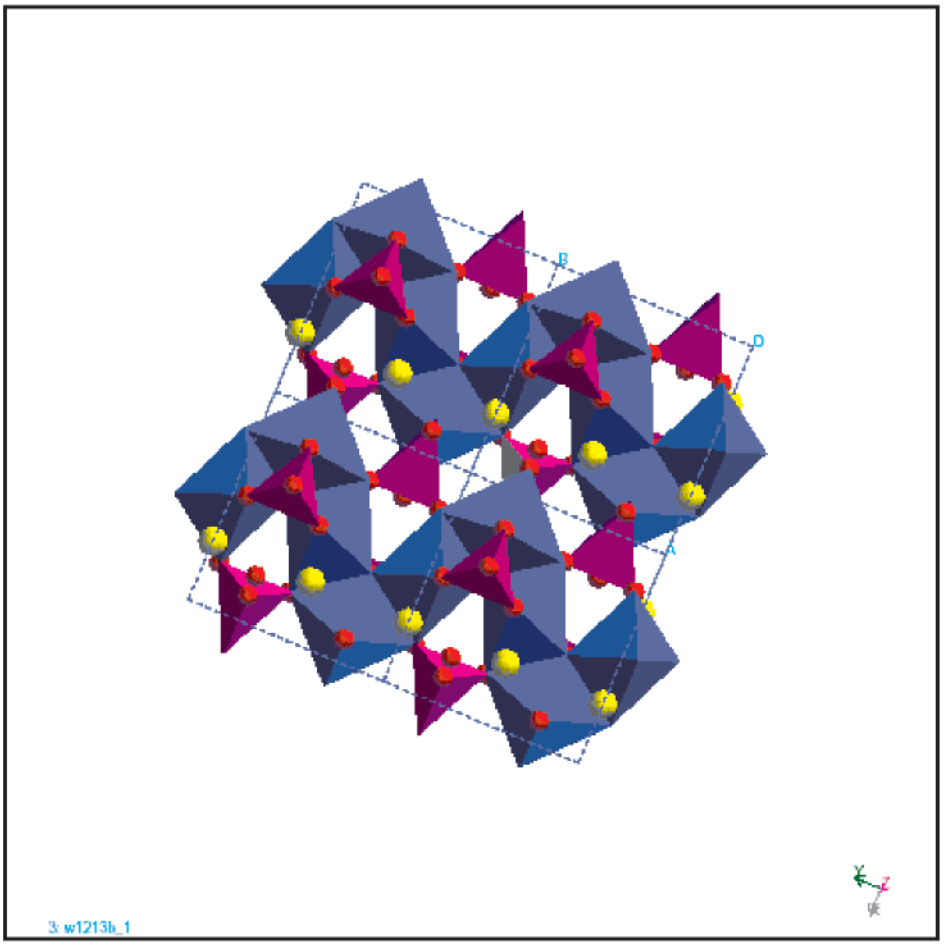

Figure 1. Projection of MPOS-3 along [001]. Oxygen and sodium atoms are represented by red and yellow spheres, respectively. Blue octahedra correspond to MnO_6 octahedra and purple tetrahedra correspond to PO_4 tetrahedra.

zigzag chains are connected by $P(3)O_4$ tetrahedra to form two-dimensional planes. A $P(3)O_4$ tetrahedron corner-shares two apexes with one zigzag chain, and edge-shares the other two apexes with a $Mn(1)O_6$ octahedron of another zigzag chain, which is another reason for the severe distortion of the Mn(1)O6 octahedra. On both sides of the two-dimensional planes, there are $P(4)O_4$ tetrahedra connecting three apexes with three MnO_6 octahedra, with the fourth apex sticking out of the plane. Sodium ions are between the two-dimensional planes of MnO_6 octahedra and PO_4 tetrahedra and interact strongly with the fourth apex of the $P(4)O_4$ tetrahedra, as shown in Figure 2. Water molecules are located in the one-dimensional microporous voids surrounded by the two-dimensional planes and sodium ions.

C. Characterization. *Powder X-ray Diffraction.* The polycrystalline MPOS-3 gives a well-defined powder XRD pattern as shown in Figure 3. The pattern is different from those of some clay and layered structural materials, which usually exhibit broader peaks and decreasing peak intensity with increasing 2θ angle.

Surface Area and Porosity. The BET surface area of MPOS-3 is 17 m^2/g, calculated from the N_2 adsorption isotherm of Figure 4. Meso- and macropores account for 10 m^2/g of this 17 m^2/g surface area. Micropore size

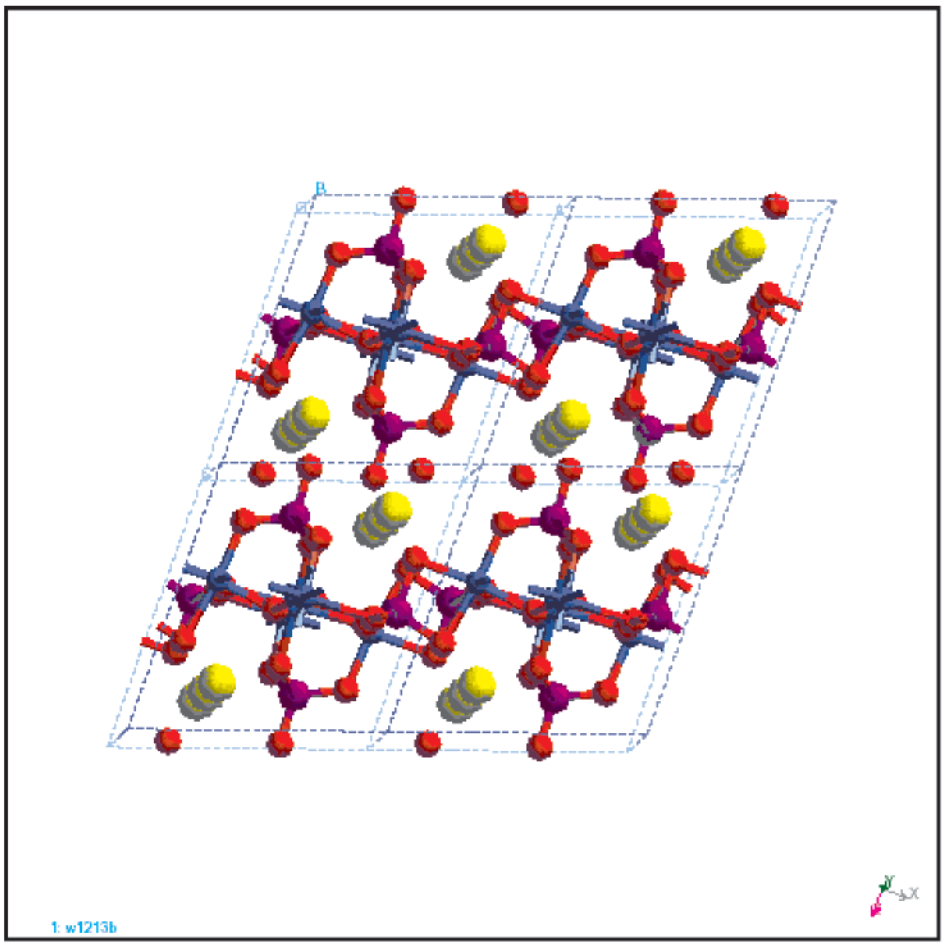

Figure 2. Perspective view of MPOS-3 along [010]. Manganese, phosphorus, oxygen, and sodium atoms are represented by blue, purple, red, and yellow spheres, respectively.

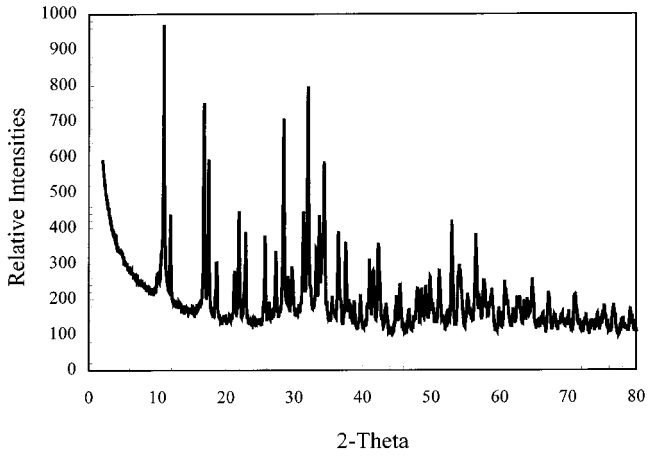

Figure 3. Powder X-ray diffraction pattern for MPOS-3.

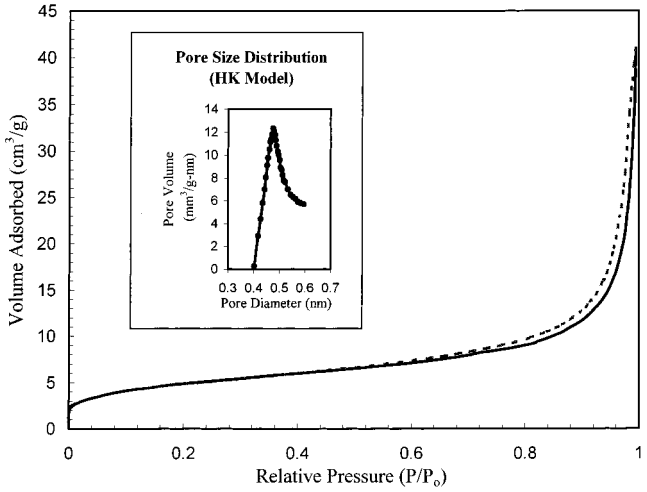

Figure 4. N_2 adsorption/desorption isotherm of MPOS-3, with the solid line for adsorption and the dashed line for desorption. Micropore size distribution of MPOS-3 is also inserted.

distributions indicate an average pore size of 4.8 Å in diameter. Adsorption data at very low relative pressure are used to calculate micropore size distribution. To obtain accurate adsorption data at very low pressure, a two-step method is employed; that is, the sample is heated under vacuum after helium gas is used to calibrate the system volume to remove any trapped helium in micropores. Ion exchanging half of the Na^+ with Ca^{2+} increases the surface area to 45 m^2/g, which is composed of 15 m^2/g micropore surface area and 30 m^2/g meso- and macropore surface area. Micropore size distributions do not show significant changes on ion exchange.

FTIR Spectrum. About 1% of MPOS-3 in weight is mixed with 50 mg of KBr and pressed into a pellet for IR studies. A transmittance spectrum is shown in Figure 5. Two distinctive −OH stretching vibration bands, one at 3437 cm^{-1} and the other at 3626 cm^{-1}, are probably associated with crystalline water. Two bands between 1080 and 1230 cm^{-1} belong to P−O

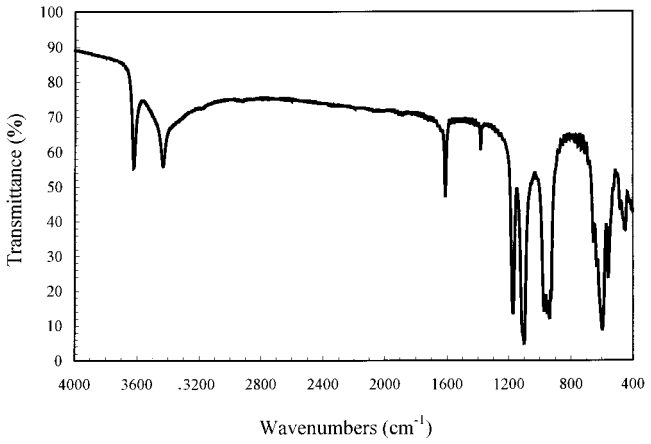

Figure 5. FTIR transmittance spectrum for MPOS-3.

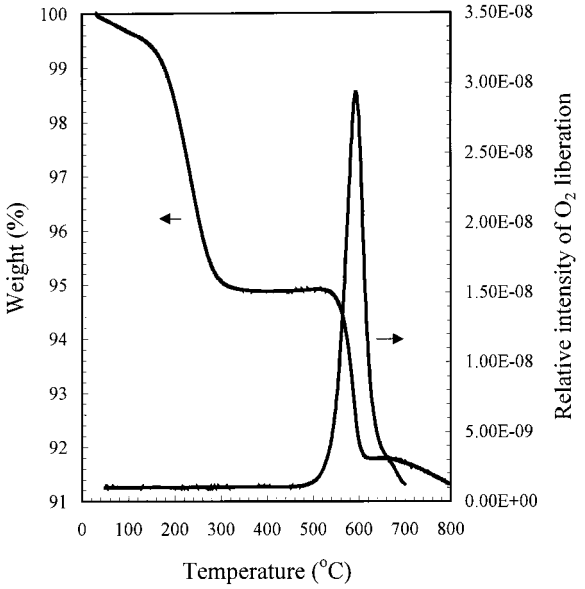

Figure 6. TGA profile and TPD decomposition profile for MPOS-3.

vibrations. Bands <700 cm^{-1} are due to Mn−O vibrations.

Thermal Stability. The TGA curve in Figure 6 shows two major weight losses. The one at about 220 °C is due to loss of crystalline water. Oxygen is liberated at 550 °C, as detected by mass spectrometry using a TPD setup.

Catalytic Activity. About 50 mg of MPOS-3 is loaded in a fixed bed reactor. Vapor of 2-propanol is carried by flowing air and helium (total flow, 12 mL/min) to the reaction zone, which is heated to 450 °C. The conversion of 2-propanol is about 27%, with 64% selectivity toward acetone and carbon dioxide as the only byproduct. In a parallel experiment, cryptomelane, a tunnel structure manganese oxide with a manganese oxidation state between 3.5 and 4.0, oxidizes 2-propanol to carbon dioxide with 100% selectivity at 200 °C.

IV. Discussion

The initial pH of the precursor mixture is adjusted to be between 3 and 4, which is not far from 6 to 7, the pH range where PO_4^{3-} coordinates to Mn^{3+}. Instant precipitation of Mn^{3+} and/or Mn^{4+} species is avoided. There are three parts in the precursor mixture, a clear 2-butanol solution, a dark red aqueous solution, and a dark brown gel. The amount of the gel increases with aging in 2−3 weeks. Presumably, TEA^+ combines with MnO_4^- to slow the reduction of MnO_4^-. This slows the formation of Mn^{3+} and/or Mn^{4+} species. The small amount of 2-butanol[18] dissolved in water may have changed the solubility of the TEA^+ species and/or the reduction path of MnO_4^-. Gel formation is also facilitated by adding 2-butanol to the precursor mixture.

Among transition-metal (oxo- and/or hydroxo-) phosphates of open structures, no edge-sharing zigzag MO_6 octahedral chain has been reported. The structure of $LiMn(OH)PO_4$,[19,20] which has the same Mn:P:O:H:Li/Na ratio as MPOS-3, has a totally different geometry. Instead, a one-dimensional tunneled framework is formed, with Li^+ residing inside the one-dimensional tunnels. The connectivity of MnO_6 octahedra in the $LiMn(OH)PO_4$ structure does not stop at one-dimensional chains. There are corner-sharing MnO_6 chains viewed from one direction, but MnO_6 octahedra also share edges in other directions, which produces the tunnels of $LiMn(OH)PO_4$ at the ends. Sodium ions are bigger than lithium ions. The one-dimensional tunnels of $LiMn(OH)PO_4$ are probably not large enough to contain Na^+, which could explain why MPOS-3 does not form a tunnel structure.

A lamellar structure is also adopted by $Ba(MnPO_4)_2 \cdot H_2O$.[14] There are no oxo groups in $Ba(MnPO_4)_2 \cdot H_2O$, and the oxidation state of manganese is 2+, and its MnO_6 octahedra share only corners to form chains. Corner-sharing chains of VO_6 octahedra are also reported in the framework of $(NH_4)VOPO_4$,[5] which has a three-dimensional open structure.

Manganese oxides with open structures can be used in total oxidation reactions of carbon monoxide[11] and benzene.[12] Edge-sharing chains and/or planes are basic features in manganese oxide open structures,[21−23] whereas only straight chains have been reported so far. Presumably, the presence of Mn−O−Mn bonds is necessary for these catalytic reactions. The oxo groups of MPOS-3 ensure the presence of Mn−O−Mn bonds, while the number of Mn−O−Mn bonds in MPOS-3 is less due to the connectivity of MnO_6 octahedra to PO_4^{3-} groups. Several patents[24,25] have reported that manganese oxo- and/or hydroxo-phosphates can be used in partial oxidative catalysis. Considering the highly distorted $Mn(1)O_6$ octahedra, the MPOS-3 structure could be catalytically active. Therefore, a probe reaction, oxidation of 2-propanol, was tested. Good catalytic properties, 27% conversion and 64% selectivity toward acetone, are obtained at the conditions described above, with carbon dioxide as the only byproduct. In the parallel experiment, cryptomelane resulted in total oxidation of 2-propanol, which is expected since the

(18) Brock, S. L.; Sanabria, M.; Suib, S. L.; Urban, V.; Thiyagarajan, P.; Potter, D. I. *J. Phys. Chem. B* **1999**, *103*, 7416−7428.
(19) Aranda, M. A. G.; Attfield, J. P.; Bruque, S. *Angew. Chem., Int. Ed. Engl.* **1992**, *31*, 1090−1092.
(20) Aranda, M. A. G.; Bruque, S.; Ramos-Barrado, J.; Attfield, J. P. *Solid State Ionics* **1993**, *63−65*, 407−410.
(21) Post, J. E.; Von Dreele, R. B.; Buseck, P. R. *Acta Crystallogr.* **1982**, *B38*, 1056−1065.
(22) Drits, V. A.; Ailvester, E.; Gorshkov, A. I.; Manceau, A. *Am. Mineral.* **1997**, *82*, 946−961.
(23) Post, J. E.; Bish, D. L. *Am. Mineral.* **1988**, *73*, 861−869.
(24) Lewis, G. J. U.S. Patent 5,780,003, 1998.
(25) Lewis, G. J.; Bogdan, P. L. U.S. Patent 6,020,533, 2000.

manganese oxidation state in cryptomelane is higher than that of MPOS-3, and there are also more Mn−O−Mn connections in cryptomelane. Detailed catalytic studies are underway.

The zigzag feature of the MnO_6 octahedral chains in MPOS-3 is unique in transition-metal phosphates. A possible explanation could be that $P(4)O_4$ tetrahedra dictate the zigzag feature by sharing three apexes with three different MnO_6 octahedra of a single chain. The zigzag chains are connected by $P(3)O_4$ tetrahedra to form two-dimensional planes. The $P(3)O_4$ tetrahedra share one edge (two apexes) with an $Mn(1)O_6$ octahedron of one zigzag chain and the other two apexes with another zigzag chain. The PO_4 tetrahedra are only slightly distorted. Therefore, the connecting points of the zigzag chains are thermally stable. Though MPOS-3 loses its crystalline water between the two-dimensional planes at 220 °C, the two-dimensional layers of MnO_6 octahedra and PO_4 tetrahedra do not lose oxygen until 550 °C. Manganese oxides[26] with open structures usually liberate oxygen between ∼300 and 400 °C. Introduction of PO_4 tetrahedral building units may have stabilized the MPOS-3 structure.

On both sides of the two-dimensional layers, there are $P(2)O_4$ tetrahedra with one apex facing outward from the layers and interacting strongly with Na^+ which resides between the layers. Stacking of the layers is therefore more rigid as compared with clay materials, which is also implied by the powder XRD pattern of MPOS-3 in Figure 3. Loss of crystalline water does not cause collapse of the MnO_6 octahedra and PO_4 tetrahedra layers, but may shift the relative positions between the layers. Ion exchanging half of the Na^+ with Ca^{2+} only expands the interlayer distance by 0.23 Å, whereas it increases the BET surface area of MPOS-3 from 17 to 45 m^2/g. Ion exchanging may cause particle size decrease, which results in the increase of meso- and macropore surface areas (from 10 to 30 m^2/g). The increase in micropore surface area (from 7 to 15 m^2/g) can be explained in two ways. First, one Ca^{2+} replaces two Na^+, which may create more voids or increase the accessibility of the one-dimensional voids. Second, ion exchange (at 90 °C) might have moved the positions of crystalline water and even slightly the positions of cations, so the one-dimensional voids are probably less occupied and slightly expanded.

The FTIR transmittance spectrum of MPOS-3 shows the absence of HPO_4^{2-} and $H_2PO_4^-$ groups. The −OH stretching bands at 3437 and 3626 cm^{-1} are probably associated with crystalline water. The dehydrated MPOS-3 only shows broad −OH stretching bands of adsorbed water in its spectrum. Ion exchanging all Na^+ with protons destroys the MPOS-3 structure. However, ion exchanging a small amount of Na^+ with protons without damaging the structure is possible and can create acidic centers, which could be catalytically useful.

V. Conclusions

Novel synthetic approaches have been developed to prepare MPOS-3, a new manganese phosphate open structure. A large number of PO_4^{3-} groups, a suitable pH, and aging time are critical for the synthesis. Tetraethylammonium cations and 2-butanol are added to ensure single-phase preparation. There exists a unique feature of zigzag edge-sharing MnO_6 octahedral chains in the MPOS-3 structure. The zigzag chains are connected by PO_4^{3-} groups to form two-dimensional planes. Water molecules and Na^+ ions reside between the planes. Ion exchanging half of the Na^+ with Ca^{2+} increases the BET surface area of MPOS-3 from 17 to 45 m^2/g. MPOS-3 is stable up to 550 °C. MPOS-3 may find catalytic applications in partial oxidation reactions, such as conversion of 2-propanol to acetone.

Acknowledgment. This work has been supported by the U.S. DOE under Contract DE-FG02-86ER13622 and Contract DE-AC02-98CH10886. Research was carried out (in part) at the National Synchrotron Light Source, Brookhaven National Laboratory, which is supported by the U.S. Department of Energy, Division of Materials Sciences and Division of Chemical Sciences. The authors thank Professor James Knox of the Biology Department of the University of Connecticut for his suggestions in structure determination. We acknowledge the support of MSI for modeling studies. The authors acknowledge Young-Chan Son for his efforts in catalytic reactions. We also thank Dr. Galasso and Dr. Gao for helpful suggestions.

CM010540A

(26) Yin, Y. G.; Xu, W. Q.; Suib, S. L.; O'Young, C. L. *Inorg. Chem.* **1995**, *34*, 4187−4193.